AIAA JOURNAL
Vol. 39, No. 5, May 2001

Aerodynamics of Gurney Flaps on a Wing in Ground Effect

Jonathan Zerihan* and Xin Zhang†
University of Southampton, Southampton, England SO17 1BJ, United Kingdom

A study was performed of a single-element, high-lift wing fitted with Gurney flaps in ground effect. The effect of the Gurney has been quantified in terms of aerodynamic performance and flowfield characteristics. The results are of direct relevance to both aeronautical and racing car applications. The qualitative performance of the Gurney in ground effect compares with freestream; the normal force of the wing is increased and a sharper stall results. Laser Doppler anemometry was used to investigate the effect of the Gurney on the turbulent wake characteristics behind the wing. Particle image velocimetry was employed to elucidate the unsteady flow behind the Gurney, which is characterized by a street of alternately shedding, discrete vortices away from the ground. When flow starts to separate from the trailing edge of the suction surface, the stall mechanism in ground effect, an unsteady wake results and the aerodynamic performance deteriorates.

Nomenclature

C_D	=	drag coefficient, $D/q_\infty c$
C_L	=	downforce coefficient directed to ground, $L/q_\infty c$
$\bar{C}_P$	=	canonical pressure coefficient, $1-(C_p-1)/(C_{pm}-1)$
C_p	=	pressure coefficient, p/q_∞
C_{pb}	=	Gurney base pressure coefficient
C_{pm}	=	pressure coefficient at maximum suction
c	=	wing chord, 223.4 mm
D	=	drag
d	=	Gurney flap height including wing trailing-edge thickness
f	=	frequency
h	=	Gurney flap height
h_r	=	ride height
h_{rm}	=	maximum downforce ride height
L	=	downforce (lift)
Re	=	Reynolds number, $\rho U_\infty c/\mu$
Sr	=	Strouhal number, fd/U_∞
s	=	distance from start of pressure-rise
s_{TE}	=	s at trailing edge
U_∞	=	freestream velocity
u, v, w	=	velocity components in x, y, z axis system
x, y, z	=	Cartesian coordinates, x +ve downstream, y +ve up, z +ve to starboard
α	=	incidence
$\Delta C_L\|_{GF}$	=	increase in downforce over a clean wing
$\Delta C_p\|_{TE}$	=	pressure difference at wing trailing edge
δ	=	wake thickness non-dimensionalised by chord, based on 99% thickness
δ_{bottom}	=	bottom of wake
δ_{clean}	=	wake thickness of clean wing
δ_{GF}	=	wake thickness of wing with 2.9% Gurney
δ_{top}	=	top of wake
μ	=	viscosity
ρ	=	density
Ω	=	vorticity, $(\partial v/\partial x - \partial u/\partial y)c/U_\infty$

Introduction

THE Gurney flap is a simple device consisting of a short strip, fitted perpendicular to the pressure surface along the trailing edge of a wing. With a typical size of 1–5% of the wing chord, it can exert a significant effect on the lift (downforce), with a small change in the stalling incidence, leading to a higher $C_{L\max}$, as documented by Liebeck.[1] Figure 1 shows a 2.9% device, fitted to the generic high-lift wing employed in this study. Although the device was named after Gurney in the 1960s, mechanically similar devices were employed earlier, for example, by Gruschwitz and Schrenk[2] and Duddy.[3]

There has been a substantial body of research on Gurney flaps over the past 20 years, most of which is concerned with aeronautical applications. The effects of Gurney flaps on aerodynamic forces and pressures were reviewed and studied in model tests by, among others, Liebeck,[1] Giguère et al.,[4] and Myose et al.[5] On the lift enhancement mechanism, there exists a variety of explanations. Liebeck[1] was the first to propose a short region of separated flow directly upstream of the Gurney flap, with two counter-rotating vortices downstream, which he described as having a turning effect on the local flowfield. He was referring to a mean flowfield. Neuhart and Pendergraft[6] observed similar vortex structures in a water tunnel, but at a relatively low Reynolds number ($Re = 8.6 \times 10^3$). At this Reynolds number, the wake of the airfoil with no Gurney flap fitted was unstable, making it difficult to identify any flow instabilities that were caused by the Gurney flaps. Thus far, Reynolds averaged Navier–Stokes (RANS) computational studies of the flow around Gurney flaps, for example, by Jang et al.[7] and more recently by Janus,[8] have given no information on any flow instabilities. Recently, Jeffrey et al.[9] and Jeffrey[10] conducted a laser Doppler anemometry (LDA) study of flow around wings fitted with Gurney flaps of various sizes. It was found that the time-averaged flow downstream of a Gurney flap consists of two counter-rotating vortices, but the instantaneous flow structure actually consists of a wake of alternately shed vortices. The vortex shedding sustains an increase in the base suction. The upstream face decelerates the flow, in a manner similar to a flat plate immersed in a turbulent boundary layer. The Gurney flap, therefore, introduces a pressure difference at the trailing edge, leading to an increase in the total circulation.

Thus far the experimental and numerical studies, although yet to present a complete picture of fluid physics, are beginning to cast light on the lift generating mechanism. Until now, nearly all of the reported studies have been with a wing/airfoil in freestream or at a high ride height. There is, however, a total lack of study/understanding of Gurney flap fluid dynamics in ground effect, with possibly the only exception of Katz and Langman,[11] for example. Yet it is in ground effect that the device has found its widest range of applications, especially on the front wing assemblies on racing cars.

When an aerodynamic device, such as a wing, operates in ground effect, the aerodynamic performance is altered, and new fluid flow features are introduced to the flow, compared with the freestream condition. The downforce (lift) generated by a wing as on a racing car front wing, at different heights from the ground has been investigated by Zerihan and Zhang.[12] The effect of the ground is to constrain the flow beneath the suction surface. At a large height in ground effect, the flow is accelerated over the suction surface to a

Received 14 October 1999; revision received 9 May 2000; accepted for publication 18 October 2000. Copyright © 2000 by Jonathan Zerihan and Xin Zhang. Published by the American Institute of Aeronautics and Astronautics, Inc., with permission.

*Ph.D. Student, School of Engineering Sciences; currently Aerodynamicist, British American Racing Operations Centre, Brackley, Northants, England NN13 7BD, United Kingdom. Student Member AIAA.

†Professor, School of Engineering Sciences. Senior Member AIAA.

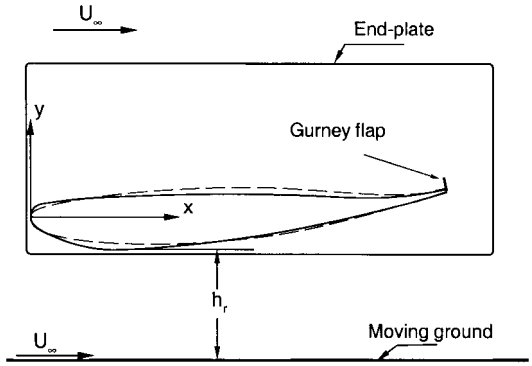

Fig. 1 Side view of Tyrrell-26 wing model with end plate and 2.9% Gurney flap and LS(1)-0413 (– – –).

greater level than in a freestream, resulting in greater suctions on the suction surface. As the wing is brought closer to the ground, flow is accelerated to a higher degree, causing an increased peak suction and associated pressure recovery. At a height where the pressure recovery is sufficiently steep, boundary-layer separation was observed at the trailing edge of the suction surface. As the height is reduced beyond this, the wing still generates more downforce, but the rate of increase slows, and the downforce reaches a maximum, the downforce reduction phenomenon. Below this height, the downforce reduces sharply. As the height is reduced from the first height where flow separation was observed, the separation point moves forward steadily. At the maximum downforce, the boundary layer separates at approximately 80%c. Heights greater than the maximum downforce are known as the force enhancement region. Below the maximum downforce is known as the force reduction region. Similarities can be drawn comparing the reduction of the height of a wing above the ground, with the increase of the incidence of a wing in a freestream. In both cases, the pressure recovery becomes steeper, eventually causing boundary-layer separation, and the wing stalls.

The flowfield established by a wing in ground effect may affect the fluid mechanics of the Gurney. Trailing-edge separation as observed in close proximity to the ground may effect the vortex shedding. The growth of the wake in terms of the unsteady effects of vortex shedding and, hence, the mean flow may be constrained by the ground. Changes in the fluid dynamics due to the ground effect will invariably lead to variations in aerodynamic performance. Under certain conditions, these will become not only performance problems but also safety issues. Therefore, it is vital to gain understanding of the fluid flow of Gurney flaps in ground effect.

It is the authors' opinion that not only can a freestream study not be applied to the situation in ground effect but also any fixed-ground studies should also be viewed with caution because different fluid flow features may exist. For fixed-ground tests, Ranzenbach and Barlow[13–15] and Ranzenbach et al.[16] found the force reduction phenomenon to be due to the merging of the wing boundary layer and the ground, in contrast to the findings of Zerihan and Zhang.[12]

This paper presents results from a recent study into the aerodynamics of the Gurney flap on a wing in ground effect. This follows an earlier study with a clean wing in ground effect. The results presented here illustrate the large-scale unsteady and time-averaged flow features caused by fitting a Gurney flap to a high-lift, single-element wing. It shows that the ground has indeed a profound effect on the fluid flow and, hence, aerodynamic performance. When associating fluid flow measurements and observation with force and pressure measurements, it is possible to develop a greater understanding of flow physics, which applies to aeronautical applications as well. In addition to the performance of the wing, the wake from the front wing of a racing car is of practical importance. The wake affects the flow to other aerodynamic devices, such as the underbody, the rear wing, and the radiators of the car.

Experimental Setup

Wind Tunnels

Experiments were performed in the University of Southampton 3.5 × 2.5 m tunnel for the LDA and particle image velocimetry (PIV) surveys and the smaller 2.1 × 1.7 m wind tunnel for the other results. Both of the tunnels are of a conventional closed-jet, closed-circuit design. For correct modeling of the ground plane, the tunnels are equipped with a large, moving belt rig, with a layout similar to that in Ref. 17. A system is located upstream of the belt for removal of the boundary layer that grows along the floor of the wind tunnel. The boundary layer is sucked away through a slot and a perforated plate. With the boundary-layer suction applied, the velocity reaches the freestream value less than 2 mm from the ground, corresponding to $h_r/c < 0.01$.

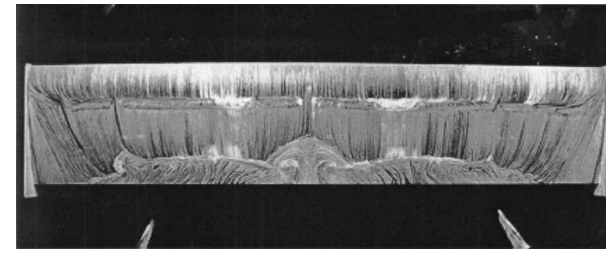

Fig. 2 Surface flow pattern on the suction surface at $h_r/c = 0.082$ and $\alpha = 1$ deg; flow from top to bottom.

Test Model

The tests were performed on a single-element, rectangular wing, untapered and untwisted, with span of 1100 mm and chord of 223.4 mm, corresponding to an aspect ratio of approximately 5. The wing profile was the main element of the Tyrrell 026 Formula 1 car front wing. The wing is a modification of a NASA GA(W) profile, type LS(1)-0413, as can be seen in Fig. 1. The main changes include a forward movement of the lowest point on the suction surface, a flattening of the pressure surface, and a modification to the leading edge. In Fig. 2, an example of the surface flow pattern on the suction surface of the wing in ground effect is shown (see later discussion). A broadly two-dimensional flow occupies the center portion of the wing.

Two sizes of Gurney flap were investigated for most tests, corresponding to heights of 1.45 and 2.9%c. Hot-wire tests were performed with 1.1, 1.4, 3.1, and 5.4%c size Gurneys. The Gurneys were formed from a brass angle section and were attached perpendicular to the pressure surface at the trailing edge of the wing, using an adhesive. Endplates were used throughout testing (Fig. 1).

Both transition-free and transition-fixed conditions were tested. Apart from fundamental interests, the tests have practical relevance as well because they are likely to correspond to the states of the flow at the beginning and end of a race, because debris is accumulated on the wing surface. Transition fixing was performed using strips of grit 1.3%c wide at an arbitrary location 10%c from the leading edge on both surfaces, using 60 grit.

Methods

The ground height was defined by the distance from the ground to the lowest point on the wing, with the wing incidence set to 0 deg. The incidence of the wing was then varied using a rotation about the quarter-chord position. All quoted incidences are measured relative to a line at 2.45 deg to the chordline. Thus, the true incidence equals quoted incidence plus 2.45 deg. Results for all of the heights and incidences were acquired for both wings with free transition and fixed transition, for the two Gurney sizes, and also the clean wing. Results presented here in ground effect are from a selection of incidences of −3, 1, 5, and 9 deg, at heights of $h_r/c = 0.045$, 0.067, 0.082, 0.090, 0.112, 0.134, 0.179, 0.224, 0.313, 0.448, 0.671, and 1.007. Freestream results were taken at incidences from −10 to 25 deg in steps of 1 deg, at a height equivalent to $h_r/c \approx 3.5$.

Lift, drag, and pitching moment data were acquired with a three-component overhead balance system. The wing was attached to the balance using a variation of the tricycle arrangement. The main struts were located at 350 mm either side of the semispan of the wing, connected at the quarter-chord position, about which the wing pivots. Behind these connection points, arms are located internally to the wing, which extend downstream and upward. A circular bar joins the two arms and connects to the pitch strut of variable length.

Flow visualization was performed transition free. A mixture of titanium dioxide and paraffin was applied to both surfaces and then was allowed to dry with the tunnel running.

Surface pressures were acquired for fixed and free transition, and for the clean wing and the wing with the 1.45% Gurney for each case.

LDA measurements were performed with a three-component Dantec system with a 5-W Ar-ion laser generator. The system was operated in backscatter mode. The velocities measured in the beam axes were resolved into the tunnel coordinate system, x, y, z, using a matrix transformation. Seeding was introduced by three seeding generators located downstream of the rolling road, behind the model. The LDA signals were analyzed using three Dantec burst spectrum analyzers. On average, a total of 800 bursts (instantaneous samples) were collected for each data point. Results were obtained for the clean wing and the 2.9% Gurney, transition fixed.

Hot-wire anemometry was used to measure the frequency of vortex shedding. A system developed locally at University of Southampton was used. Tests were performed in freestream, for the clean wing and the Gurneys, at an incidence of 1-deg, transition fixed. Data were typically taken over 1 s, and results were then processed for the frequency domain.

PIV studies, using a Dantec PowerFlow system, have been performed on the wing tested in ground effect, with fixed transition. The wing was tested clean and also with the 2.9% Gurney. The laser for the PIV system was located approximately 1.5 m downstream of the center of the wing, after the end of the rolling road. The camera was mounted outside the wind tunnel, perpendicular to the light sheet. Chordwise measurements at the wing semispan were obtained, extending from the wing to the ground and capturing the downstream flow.

The wind and belt velocities were limited to 30 m/s for all results presented here, corresponding to a Reynolds number of approximately 0.45×10^6 based on the chord.

The wind-tunnel model corresponds to 80% of the scale of the wing on the car. Current wind-tunnel testing of entire racing cars is performed using models not greater than 50% scale, at speeds of not more than 40 m/s. Although the Reynolds number of the current tests may seem low for aeronautical applications, the reference speed and model size correspond to Reynolds numbers in the range approximately 20–50% higher than current racing car testing applications.

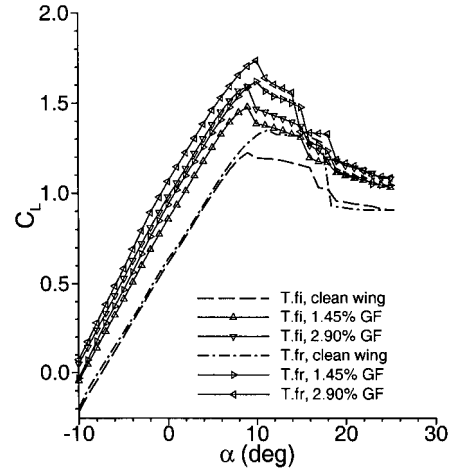

a) Lift curves

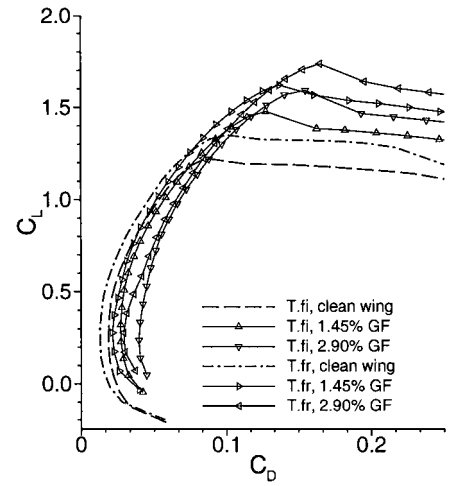

b) Drag polars

Fig. 3 Forces in freestream.

Errors and Uncertainties

The errors and uncertainties were estimated for the force results. The incidence of the wing was set to ± 0.005 deg, and the height above ground was set to ± 0.2 mm. The tunnel speed was run at a constant dynamic pressure of 56.25-mm water ± 0.05 mm. When procedures detailed by Moffat[18] are used, the uncertainties in C_L were calculated using the addition method and a 95% confidence, with the worst case occurring at a height of $0.056c$ and corresponding to a C_L of 1.678 ± 0.009. Repeatability was found to be excellent.

Uncertainties in the surface pressure results obtained using the Zoc transducer were estimated taking into consideration the same parameters such as wing height, incidence, and variation in dynamic pressure. The quoted transducer uncertainty as well as the calibration offsets after the end of the run were included. The uncertainties were calculated for the individual tappings using the root-sum-square method as described by Moffat,[18] with the worst case corresponding to the tapping at $x/c = 0.336$ and a C_p of ± 0.035. The short-term repeatability was investigated; the highest uncertainties were found to be at the suction peak and the transition bubble and the worst corresponding to a C_p of ± 0.075 at $x/c = 0.134$.

Results and Discussion

Forces in Freestream

As a baseline case, the forces in the freestream were measured. The lift curves can be seen in Fig. 3. The results suggest that fitting a Gurney increases C_L at zero incidence and has a negligible effect on the stalling angle, leading to an increase in $C_{L\max}$.

For the transition-fixed case, the wing stalls at $\alpha = 9$ deg, for the clean wing and the two Gurneys. This is the angle at which trailing-edge separation starts to occur. The plateau in the C_L beyond this occurs as the separation point moves forward until it reaches the leading edge, at $\alpha = 17$ deg for the clean wing and $\alpha = 16$ deg for the two cases with the Gurneys, as can be seen in Table 1. The smaller Gurney has a disproportionately large effect on the force increment. This was pointed out by other researchers as well, for example, Myose et al.[5] and Jeffrey.[10] The stall of the wing becomes sharper with the addition of the Gurneys. Flow separation at the suction surface trailing edge causes a disturbance to the vortex shedding behind the Gurney, leading to a partial loss in performance of the Gurney. Note that the spacing between the measurement points was typically 1 deg, which gives an indication of uncertainties in the results.

For the transition-free case, boundary-layer transition on the suction surface appears at approximately $0.3c$ (see Zerihan and Zhang[12] and later C_p results). The stalling incidence of the wing increases from $\alpha = 9$ to 11.3 deg for the clean wing, when compared with the transition-fixed flow. The boundary layer is thinner, and, hence, flow separation will occur at a higher incidence, compared to the transition-fixed results. The Gurneys slightly reduce the incidence at which the trailing-edge separation occurs (from 11.3 to 10 deg).

The gain in C_L with the addition of the Gurney from the clean wing increases with incidence (Fig. 3 and Table 1) for both the transition-fixed and transition-free conditions. This causes a nonlinear lift slope, decreasing with incidence. The mean value for the lift slope, however, increases with the Gurney added. The smaller Gurney is seen to have a disproportionately large effect on the lift slope increase. These characteristics have been described by Jeffrey.[10] Similar observations can be made of the zero-force incidence reduction.

Drag polars are plotted in Fig. 3b, with zero lift drag coefficients listed in Table 1. For most values of C_L (up to a critical value)

Table 1 Aerodynamic performance of wing in freestream

GF height h/c, %	$dC_L/d\alpha$, rad^{-1}	α_0, deg	$C_{L\max}$	$\Delta C_{L\max}$ over clean wing, %	C_{D0}	$\alpha_{TE\ stall}$, deg	$\alpha_{LE\ stall}$, deg
Clean[a]	4.73	−7.45	1.22	——	0.0240	9.0	17.0
1.45[a]	5.29	−9.50	1.48	21	0.0372	9.0	16.0
2.90[a]	5.57	−10.52	1.59	30	0.0472	9.0	16.0
Clean[b]	4.57	−7.84	1.35	——	0.0187	11.3	18.4
1.45[b]	5.38	−9.69	1.62	20	0.0354	10.0	16.0
2.90[b]	5.73	−10.72	1.74	29	0.0419	10.0	15.0

[a]Transition fixed. [b]Transition free.

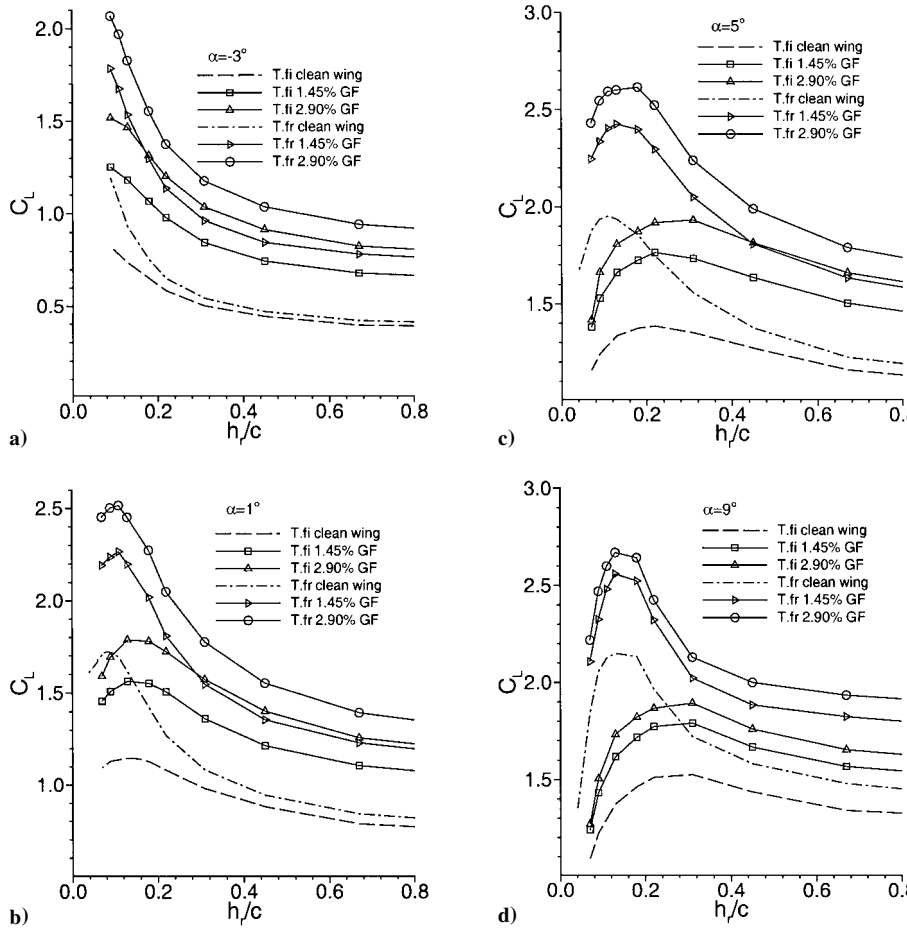

Fig. 4 Downforce coefficients vs ride height.

the Gurneys increase the drag. Above the critical value, the Gurney produces a small reduction in drag.

Forces in Ground Effect

The force coefficients at $\alpha = -3$, 1, 5, and 9 deg are presented for a variety of heights in Fig. 4. Of the four incidences, $\alpha = -3$ deg represents a limiting case in the linear range; $\alpha = 1$ and 5 deg represent normal incidence settings; $\alpha = 9$ deg is associated with the onset of the trailing-edge separation. With a reduction in the ground height, from far from the ground, the downforce typically experiences an enhancement and then a reduction, as described briefly in the Introduction and more completely in Ref. 12. The onset of force reduction is triggered by the trailing-edge separation on the suction surface. As the ride height is reduced, the extent of the trailing-edge separation increases. At $\alpha = 1$ deg, the greatest height at which separation is observed is approximately $h_r/c = 0.224$, for the clean wing, transition free. At this height, the rate of force enhancement starts to slow down with the reduction in ride height, until a peak is reached at $h_r/c \approx 0.08$. The force then drops with the reduction in ride height. Figure 2 shows an example of the trailing-edge flow separation on the suction surface in this region.

Similar characteristics are seen for the transition-fixed case at the same incidence (Fig. 4b). The force reduction phenomenon, however, occurs at a greater height and corresponds to a significantly lower downforce than for the transition-free case, as described by Zerihan and Zhang.[12] Transition fixing causes a thicker boundary layer, that is, a boundary layer that is closer to separation compared to the transition-free case, for an arbitrary height. Hence, as the wing is brought closer to the ground from large ground heights, the boundary-layer separation and subsequent loss in circulation will occur at a greater height for the transition-fixed case than for transition-free case. The Gurney has a similar effect in terms of aerodynamic performance for the transition-fixed case compared to the transition-free case.

Figure 4 highlights the ground effect of the various configurations at the other incidences. Increasing the incidence of the wing causes a reduction in sensitivity to ground height[12] in terms of both downforce gain from large heights to the maximum downforce and also rate of change of downforce with respect to ride height in the force enhancement region. For the lowest incidence (Fig. 4a), the geometry of the endplates did not allow testing at very close proximity to the ground, and the force reduction phenomenon cannot be seen.

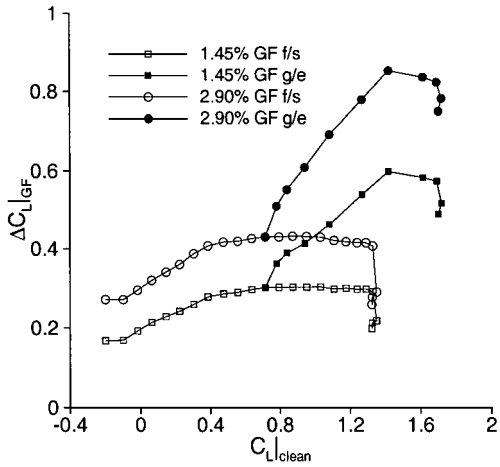

Fig. 5 Increase in downforce with Gurneys in freestream and ground effect, transition free.

For the wing far from the ground, if the wing incidence is increased, separation is more likely to occur. As the ride height is reduced, the boundary layer will separate at a greater height for the wing at a higher incidence than for the lower incidence, causing a greater subsequent loss in downforce. The rate of increase of downforce as the ground is approached is, therefore, smaller for the higher incidence than for the lower incidence, leading to a lower overall gain in downforce for the higher incidence case. A tendency is also seen for the maximum downforce to occur at a greater height as the incidence is increased. Again, the effect of the Gurney is similar for the cases as the incidence is changed in terms of the aerodynamic performance.

Figure 5 presents the gain in downforce with the Gurney compared to the clean wing, $\Delta C_L|_{GF}$, with the downforce for the clean wing, for the transition-free case. These plots have been used to show that the downforce gain with the Gurney is a function of the downforce for the clean wing, not the wing profile,[10] for a wing in freestream. Jeffrey's results[10] show that the points collapse onto the same line for a particular size Gurney, for different wings: a NACA0012 and a high-lift e423. The current results are presented for a freestream, where the wing incidence has been varied, and for ground effect, where the ride height has been varied at $\alpha = 1$ deg. It is clear that the results for the freestream and the ground effect are significantly different. In ground effect, adding a Gurney flap increases the downforce more significantly than in the freestream.

In the force enhancement region, as $C_{L\text{clean}}$ is increased to 1.42, $\Delta C_L|_{GF}$ increases as the ground is approached. At the corresponding height from the ground, $h_r/c = 0.179$, surface flow visualization, surface pressure surveys, and PIV studies (see later sections) all indicate that this is the height at which the the boundary layer starts to separate from the suction surface. As the height is reduced to that at which the maximum downforce occurs, corresponding to $C_L = 1.72$, the $\Delta C_L|_{GF}$ reduces. This trend continues in the force reduction region. The reduction in performance of the Gurney is attributed to the flow separation, the size of which increases as the height is reduced.

Chordwise Pressures

Surface pressures were measured at an incidence of $\alpha = 1$ deg for both transition-free and transition-fixed conditions, with the 1.45% Gurney.

Results in Fig. 6a show the pressure distributions at different heights from the ground, for the transition-free case. The effect of changing the height from the ground on the pressure distribution is similar to earlier results using the clean wing.[12] As the ground height is reduced, the pressure is reduced slightly on the pressure surface. A more significant increase in suction is found on the suction surface. For all ground heights, the peak suction on the suction surface increases as the ground height is reduced. The associated pressure recovery increases, and the boundary layer comes nearer to separation. For the results shown at the smallest height from the

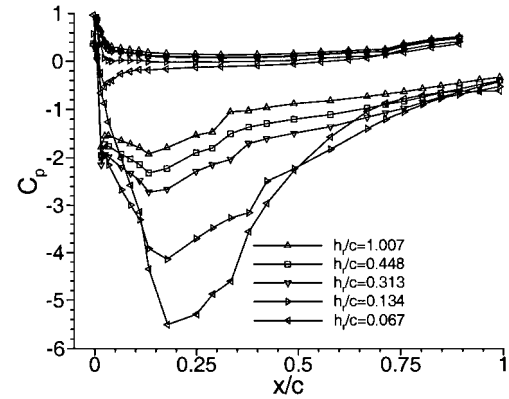

a) 1.45% Gurney flap

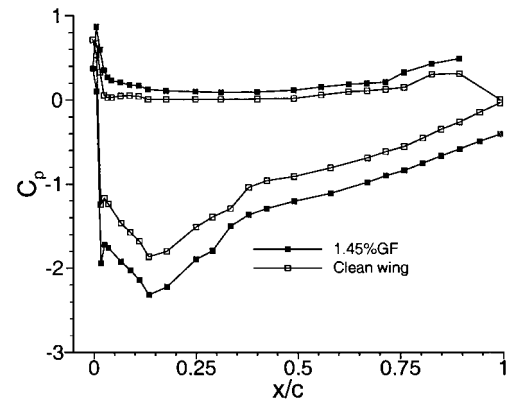

b) At $h_r/c = 0.448$

Fig. 6 Pressure coefficients at $\alpha = 1$ deg transition free.

ground, $h_r/c = 0.067$, a significant area of flow separation is evident near to the trailing edge, as illustrated by the constant pressure region. This results in a loss of circulation over the rear portion of the wing.

Figure 6b shows the effect of adding the Gurney, for a height of $h_r/c = 0.448$, again transition free. Although the final point on the pressure surface has not been included, due to being covered by the Gurney, the finite pressure difference at the trailing edge can be observed. The Gurney retards the flow over the pressure surface, as illustrated by the increase in pressure. Over the last 30%c of the pressure surface, however, the increase in pressure is greater than for farther upstream of this. Greater suctions are found over the entire suction surface. The increment in suction is also seen to increase over the final 30%c, from 0.29 at $x/c = 0.72$ to 0.32 at $x/c = 0.85$ and 0.36 at $x/c = 0.99$. The increase in suction at the trailing edge is associated with the vortex shedding mechanism.[10] Both the increase in pressure surface pressures and suction surface suctions cause the increase in downforce with the Gurney.

The increase in Gurney performance in ground effect (Fig. 5) can be further discussed using the results in Fig. 7. The variation of pressure difference at the trailing edge with ground height is shown, for the transition-free case. The pressure difference has been calculated using the final pressure tappings on each surface: at $x/c = 0.99$ for the suction surface and $x/c = 0.90$ on the pressure surface. Because of the Gurney covering the final tapping on the pressure surface, the results can only be compared quantitatively. It can be seen that, as the ground height is reduced, the pressure difference increases from 0.89 at $h_r/c = 0.671$ to 0.94 at $h_r/c = 0.224$ to a maximum of 1.06 at $h_r/c = 0.113$. Closer to the ground than this, the pressure difference drops steadily.

Suction Surface Canonicals

Canonical pressures[19] are useful in separation analysis, allowing pressure recoveries to be compared directly as long as the Reynolds numbers based on the momentum thickness at the start of the pressure recoveries are similar. It is shown that the boundary layer will separate at a given canonical pressure, when comparing

Table 2 Wake characteristics

Test case								
Wing	h_r/c	x/c	u_{min}/U_∞	y at u_{min}	y at δ_{top}	y at δ_{bottom}	δ	$\delta_{GF}-\delta_{clean}$
Clean	0.448	1.5	0.83	0.08	0.12	0.05	0.07	0.09
Clean	0.448	2.0	0.92	0.09	0.15	0.05	0.10	0.09
Clean	0.448	3.0	0.93	0.11	0.18	0.05	0.13	0.13
Clean	0.224	1.5	0.79	0.06	0.11	0.01	0.10	0.11
Clean	0.224	2.0	0.88	0.08	0.14	0.01	0.13	0.12
Clean	0.224	3.0	0.93	0.11	0.18	0.01	0.17	0.15
Clean	0.134	1.5	0.77	0.04	0.11	−0.04	0.15	0.09
Clean	0.134	2.0	0.85	0.04	0.13	−0.06	0.19	0.13
Clean	0.134	3.0	0.91	0.05	0.18	−0.07	0.25	0.18
2.90%GF[a]	0.448	1.5	0.82	0.13	0.20	0.04	0.16	
2.90%GF	0.448	2.0	0.85	0.17	0.24	0.05	0.19	——
2.90%GF	0.448	3.0	0.88	0.22	0.33	0.06	0.26	——
2.90%GF	0.224	1.5	0.80	0.14	0.22	0.01	0.20	——
2.90%GF	0.224	2.0	0.81	0.15	0.24	0.00	0.24	——
2.90%GF	0.224	3.0	0.86	0.19	0.33	0.01	0.32	——
2.90%GF	0.134	1.5	0.72	0.07	0.20	−0.04	0.24	——
2.90%GF	0.134	2.0	0.77	0.09	0.22	−0.10	0.32	——
2.90%GF	0.134	3.0	0.82	0.13	0.33	−0.10	0.43	——

[a]Gurney flap.

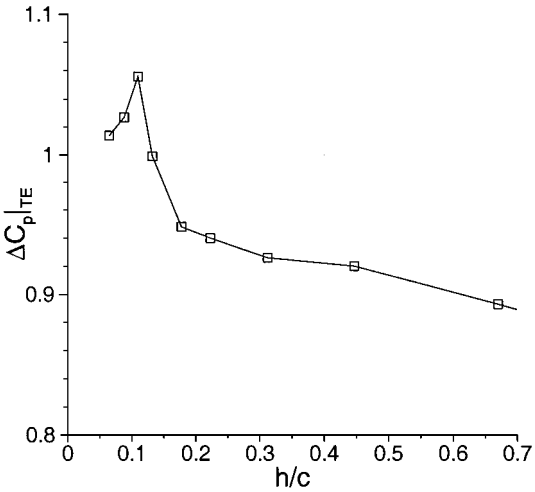

Fig. 7 Pressure difference at trailing edge for 1.45% Gurney at α = 1 deg, transition free.

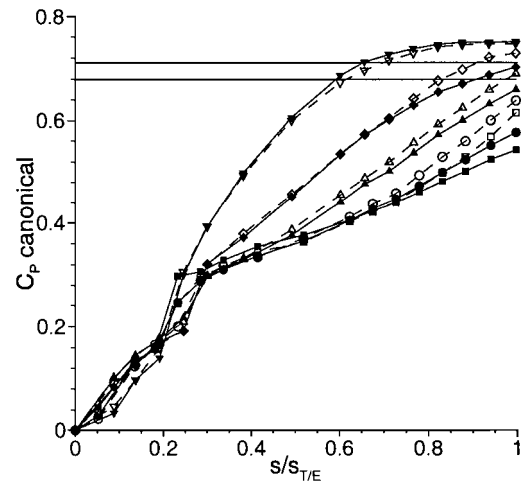

Fig. 8 Suction surface canonicals at $\alpha = 1$ deg, transition free: ▽ and ▼, $h_r/c = 0.067$; ◇ and ◆, $h_r/c = 0.134$; △and ▲, $h_r/c = 0.224$; ○ and ●, $h_r/c = 0.448$; and □ and ■, $h_r/c = 1.007$; and solid symbols, Gurney.

appropriate recoveries. The suction surface pressure recoveries for the transition-free cases with the 1.45% Gurney have been replotted in their canonical form, as can be seen in Fig. 8 from the solid symbols. The range of values of $\bar{C}_P = 0.68$–0.71 was obtained[12] as the canonical pressure at which the boundary layer separates. It can be seen that, for the first portion of the pressure recovery, to $s/s_{TE} \approx 0.3$, the canonical pressures decrease with increasing ground proximity. A more significant increase in canonical pressure with increasing ground proximity is seen for the remaining portion of the recovery. For the largest ground height, the pressure recovery is initially small, but increases as the trailing edge is approached. As the ground height is reduced to the $h_r/c = 0.224$ case, the pressure recovery appears broadly constant. With increasing ground proximity, the initial part of the second portion of the pressure recovery increases, but then falls off near to the trailing edge as the flow separates. The effect of the Gurney on $\bar{C}_P$ is to reduce the pressure recovery demands, causing a reduction in the canonical pressure at the trailing edge. The effect is that flow will start to separate at a smaller height for the wing with the Gurney, compared with the clean wing.

Off-Surface Flow Measurements

Mean Flow Results

Wake surveys, highlighting the effect of the Gurney on the u/U_∞ mean velocities are shown in Fig. 9, for stations at $x/c = 1.5$, 2, and 3 at a height of $h_r/c = 0.134$. Detailed information from the wake surveys at three heights, with and without the Gurney flap, is presented in Table 2. Note the coordinates of the wing trailing edge are $x/c = 1.0$ and $y/c = 0.06$.

Adding the Gurney flap to the wing causes a larger wake in terms of the thickness of the wake and the maximum velocity deficit. At $x/c = 1.5$ for $h_r/c = 0.134$ in Fig. 9a, the thickness of the wake has been measured as $\delta = 0.15c$ for the clean wing, compared to $\delta = 0.24c$ for the wing with the Gurney. The maximum velocity deficit is $u/U_\infty = 0.77$, compared to 0.72 for the clean wing and wing with Gurney, respectively. The height of this minimum velocity increases from $y/c = 0.04$ to 0.07 with the Gurney flap, as the Gurney flap has deflected the path of the wake. Although the location of the top of the wake thickness increases from $y/c = 0.11$ to 0.20, the location of the bottom remains at -0.04.

Farther downstream, at the $x/c = 2.0$ and 3.0 locations for $h_r/c = 0.134$, the effect of the Gurney is similar. Small-scale turbulence has diffused the wake of the wing such that the wakes are thicker and the maximum velocity deficits are reduced. The Gurney still has the effect of reducing the minimum velocity and increasing the height of the location thereof. This changes from $y/c = 0.04$ to 0.09 at $x/c = 2.0$ to 0.05 and 0.13 at $x/c = 3.0$. The velocities reduce from $u/U_\infty = 0.85$ to 0.77 and from 0.91 to 0.82 at the two positions. This shows that the wake is deflected through a higher angle with the Gurney. The location of the top of the wake thickness increases significantly with the Gurney: 0.13 to 0.22 at $x/c = 2.0$ and 0.18 to 0.33 at $x/c = 3.0$. The bottom of the wake grows less

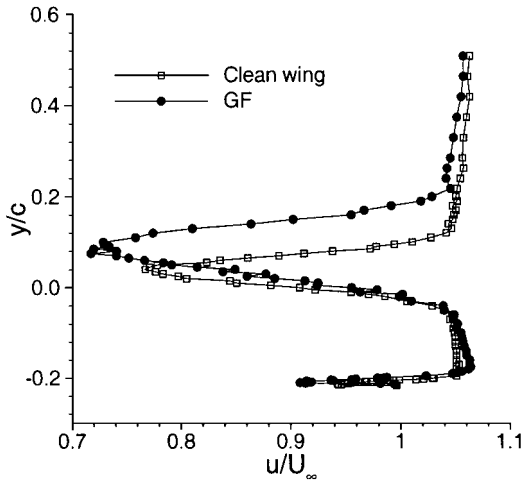

a) $x/c = 1.5$

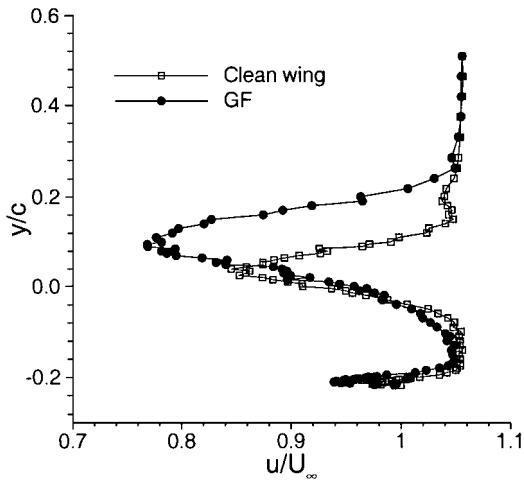

b) $x/c = 2.0$

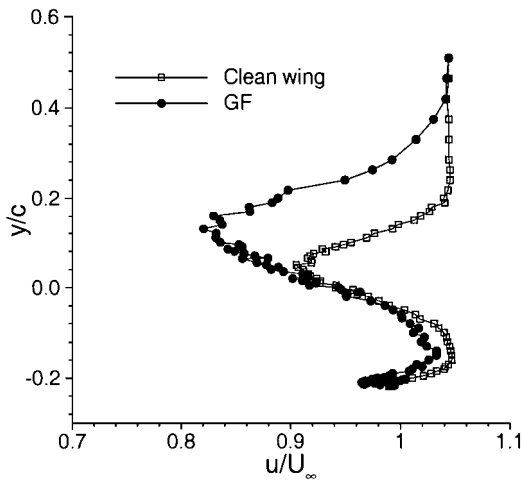

c) $x/c = 3.0$

Fig. 9 Wake characteristics behind the 2.9% GF; mean u/U_∞ profiles at $h_r/c = 0.134$.

significantly: from −0.06 to −0.10 and from −0.07 to −0.10 at the two x/c positions.

Results for the clean wing show that the wake thickness increases from $\delta = 0.15$ to 0.19 and 0.25 at the three positions at this height. This compares to thicknesses of $\delta = 0.24$, 0.32, and 0.43 for the wing with the Gurney. The increases in wake thickness when the Gurney is added are 0.09, 0.13, and 0.18, respectively. A significant result on the overall flowfield is that, when the Gurney is added, in addition to increasing the size of the wake, the wake grows at a greater rate, in terms of the distance traveled downstream. That is, $\delta_{GF} - \delta_{clean}$ increases with streamwise distance, for a given ride height. This trend can also be seen in the results for the other heights, at $h_r/c = 0.448$ and 0.224, in Table 2.

The other trends of the path of the wake being deflected though a higher angle can be seen examining the locations of the maximum velocity deficit with and without the Gurney, for the other heights tested. For example, at $h_r/c = 0.448$, this increases height from $y/c = 0.08$, 0.09, and 0.11 for the clean wing to 0.13, 0.17, and 0.22 for the wing with the Gurney.

Figure 9 is also of interest regarding the accelerated fluid between the wing wake and the ground. The results for the Gurney highlight an adverse pressure gradient in the streamwise direction. At the wing trailing edge, the flow is at an accelerated level and then retards as it moves downstream. However, for the clean wing, this adverse pressure gradient seems to be very small or negligible in Fig. 9. The velocity at the trailing edge for the clean wing is very close to the freestream level. This highlights the finite pressure difference at the trailing edge for the wing with the Gurney, associated with vortex shedding.

The general effect of the ground proximity is to increase the size of the wake (see Table 2). As the ground height is reduced, the peak suction increases, and the associated pressure recovery becomes steeper on the suction surface. This causes a thicker boundary layer and, hence, a thicker wake. In addition to this, the path of the wake reduces as the ground is approached and the wake thickens.

The general effect of the Gurney on the wake of the wing can be seen represented by the greater size of the wake and also by the well-documented turning effect.

Vortex Shedding: Hot-Wire Anemometry

Tests using hot-wire anemometry were used for an accurate assessment of the vortex shedding frequency, in the freestream. Results for the frequency response spectra indicate sharp, single peaks at periodic frequencies. Table 3 lists the results for the frequency of vortex shedding. It can be seen that increasing the size of the Gurney reduces the frequency of vortex shedding, as described by Jeffrey.[10] The Strouhal number Sr has also been calculated. As the Gurney size is increased, the Strouhal number increases asymptotically, to a value of 0.190 for the largest Gurney. This compares qualitatively with Jeffrey, where Strouhal numbers in the range 0.08–0.15 were found from LDA surveys on an e423 wing. Bearman and Trueman's study[20] quantifies the effect of the base pressure coefficient on the Strouhal number for alternately shed vortices behind a bluff body. It was found that, as the factor $K = [1 - C_{pb}]^{1/2}$ is increased, the Strouhal number reaches a constant value of $Sr = 0.181$ for $K > 1.16$. For the current results, the value of K corresponding to the 3.1% Gurney flap is approximately 1.20, to give a Strouhal number of 0.178, comparing well with Bearman and Trueman's results.

Vortex Shedding: PIV

PIV measurements were made at a number of heights at $\alpha = 1$ deg. The purpose is to provide an understanding of the vortex shedding behind the Gurney in the near-wake region, in ground effect. Selected instantaneous vorticity distributions are presented in Fig. 10. These results suggest that the vortex shedding process is altered with the wing at heights close above and also below the maximum downforce, leading to a deterioration in aerodynamic performance. The results in the top-left-hand corner of Fig. 10 have been obscured by a reflection from part of the model support arrangement.

At moderate and large heights in the force enhancement region, the boundary layer remains fully attached. The fluid mechanism of flow separation is observed for heights near to and below the force reduction phenomenon, as discussed in preceding sections, in

Table 3 Vortex shedding frequency

GF[a] h, mm	f, Hz	Sr
2.4	1064	0.144
3.2	938	0.152
6.9	623	0.178
12.2	412	0.190

[a]Gurney flap.

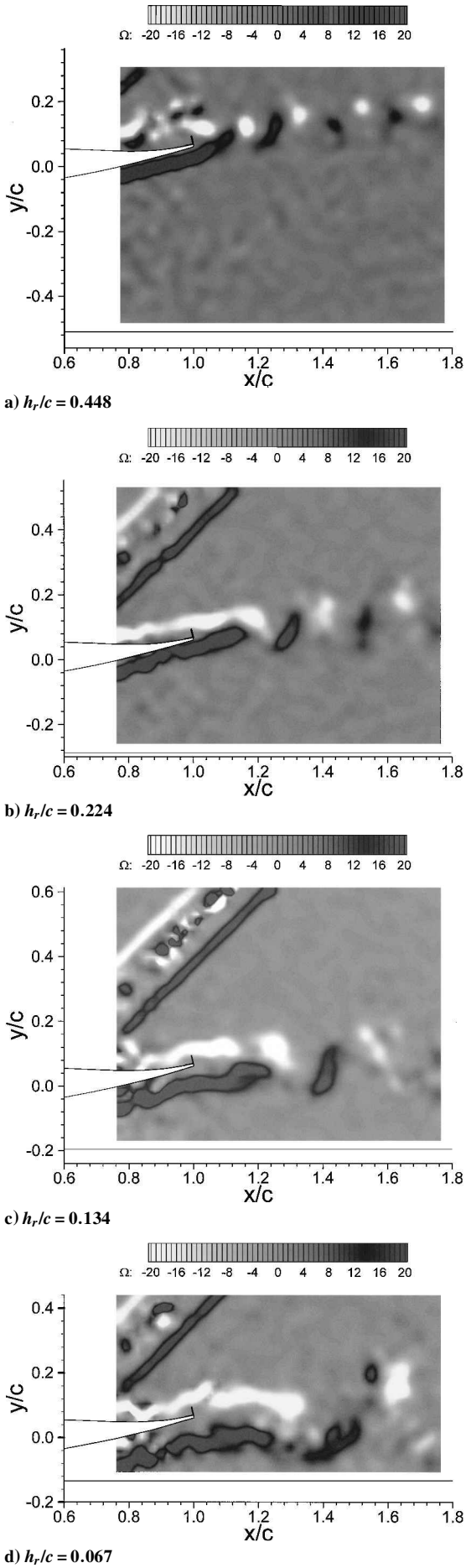

Fig. 10 Vortex shedding behind the Gurney; instantaneous vorticity contours.

a manner similar to the clean wing. Where this occurs, the gain in downforce when the Gurney is added, $\Delta C_L|_{GF}$, reduces. For large-scale flow separation, the wake size increases, and the wake is highly unsteady, as can be seen in Figs. 10c and 10d.

When the wing is placed in the force enhancement region and close above the maximum downforce, discrete vortices are generated behind the Gurney. This feature can be seen clearly in Figs. 10a and 10b, where the vortices are seen in the form of vorticity concentrations, which convect alternately downstream. Similar discrete vortices were observed at a low Reynolds number of 8.6×10^3 by Neuhart and Pendergraft,[6] though in their case the wake itself was unsteady. Jeffrey,[10] while detecting a stationary counter-rotating mean vortex pair behind a Gurney in freestream using LDA, has shown the existence of a discrete frequency by performing a frequency analysis of LDA data. The current study now shows for the first time the existence of alternately shedding vortices at a moderate Reynolds number. The suction enhancement mechanism of the alternately shed vortices, therefore, still remains in ground effect. Furthermore, in the force enhancement region, the effect of the moving ground is to increase the suction level on the suction surface near the trailing edge, which further increases the suction enhancement effect of the Gurney.

With the separation off the suction surface in the force reduction region, the mechanism by which a two-dimensional vortex-shedding flow separates to form two shear layers of opposite vorticity and then interacting to form a von Kármán vortex street, as postulated by Gerrard,[21] is absent in the immediate vicinity downstream of the Gurney. This feature is obvious in Figs. 10c and 10d. It is known that the flow entrainment process induced by the alternately shedding vortices sustains the increased base suction of bluff bodies as well as Gurneys (see Bearman[22] and Jeffrey[10]). The flow separation encountered in the trailing-edge region on the suction surface leads to a deterioration of the circulation enhancement effect of the Gurney and a reduction in the effectiveness of the device in the force reduction region, as can be seen in Fig. 4. This is manifested as an absence of discrete vortex shedding behind the Gurney flap.

Instead of alternately shedding vortices, Figs. 10c and 10d show two shear layers, one caused by the fixed separation at the off-surface edge of the Gurney on the pressure surface side and another by the separation on the suction surface, whose position moves upstream. A feature of the observed flow is the existence of high-level concentrations of vorticity in the shear layer. The vorticity concentrations are produced by the shear layer instability, which produces flapping motion leading to mass entrainment into the wake. In the current flow, the amplification of the instability waves also lead to nonlinear rollup of the shear layer, that is, large vortices. This feature can be observed at approximately $0.3c$ downstream of the wing trailing edge at $h_r/c = 0.067$ and $0.2c$ at $h_r/c = 0.134$. The shear layer thus experiences a coupled motion of flapping in the transverse direction and vortex convection in the streamwise direction. The vorticity patterns in Figs. 10c and 10d reflect this mechanism.

Another feature of practical importance is the rapid breakdown of this transverse flapping motion in ground effect. At about $0.5c$ downstream of the trailing edge at $h_r/c = 0.067$, the two layers of vorticities breakdown. This is clearly seen in Fig. 10d. In the mean flow, it manifests in the form of expanded turbulent wake. Observations of successive PIV images suggest the wake actually interacts with the ground in this process. This is significant in engineering applications because it would adversely affect performance of trailing aerodynamic devices.

Conclusions

An investigation was performed of a generic wing fitted with a Gurney flap in ground effect. By combining flow visualization, force, pressure, and velocity measurements, it was possible to identify major fluid flow features governing the fluid flow behind the wing and the Gurney flap and to assess changes in aerodynamic performance.

The following paragraphs summarize the findings:

The aerodynamic performance of the Gurney on a wing in ground effect has similar effects when compared with a Gurney on a wing in a freestream. The Gurney increases the downforce, with small

Gurneys increasing the downforce disproportionately more than a large Gurney. As the height is reduced in the force enhancement region for fully attached flow, the increase in downforce with the Gurney increases. This compares with results when the incidence of the wing is increased in a freestream. However, the gain in downforce with the Gurney in ground effect can be twice the gain in the freestream. The onset of flow separation causes a sharper stall in ground effect (the force reduction phenomenon), again similar to a freestream.

The mean flow characteristics as found from LDA results show that the wake is significantly larger for the wing with the Gurney, when compared with the clean wing. In addition to this, the wake thickens at a greater rate than for the clean wing. The turning effect of the Gurney was observed. As the height of the wing is reduced in ground effect, the wake thickens. The deflection of the wake reduces.

A vortex shedding Strouhal number of $Sr \approx 0.18$ was recorded from hot-wire tests in a freestream, which compares to that found in vortex shedding from bluff bodies.

The flow behind a Gurney flap is characterized by a street of alternately shedding, discrete vortices when the flow is fully attached, as shown by instantaneous flowfield observed with a PIV system.

In the force reduction region and at heights closely above the maximum downforce, separation occurs on the suction surface near the trailing edge, leading to an unsteady wake and altering the shear layer separated at the off-surface edge of the Gurney. The aerodynamic performance of Gurney flaps deteriorates.

Acknowledgments

J. Zerihan is supported by an Engineering and Physical Sciences Research Council studentship. The authors would like to thank W. Toet and D. Jeffrey of British American Racing for his support and discussions. Technical assistance was given by the Tyrrell Racing Organisation and British American Racing. A. Barr performed the hot-wire tests and his assistance is appreciated, in addition to all staff at the University of Southampton wind tunnels.

References

[1]Liebeck, R. H., "Design of Subsonic Airfoils for High Lift," *Journal of Aircraft*, Vol. 15, No. 9, 1978, pp. 547–561.

[2]Gruschwitz, E., and Schrenk, O., "Über eine Einfache Möglichkeit zur Auftiebserhöhung von Tragflügeln," *Zeitschrift für Flugtechnik und Motorluftschiffahrt*, No. 20, Oct. 1932, pp. 597–601.

[3]Duddy, R. R., "High Lift Devices and Their Uses," *Journal of the Royal Aeronautical Society*, Vol. 53, No. 465, 1949, pp. 859–900.

[4]Giguère, P., Lemay, J., and Dumas, G., "Gurney Flap Effects and Scaling for Low-Speed Airfoils," AIAA Paper 95-1881, June 1995.

[5]Myose, R., Papadakis, M., and Heron, I., "Gurney Flap Experiments on Airfoils, Wings, and Reflection Plane Model," *Journal of Aircraft*, Vol. 35, No. 2, 1998, pp. 206–211.

[6]Neuhart, D. H., and Pendergraft, O. C., Jr., "A Water Tunnel Study of Gurney Flaps," NASA TM 4071, Nov. 1988.

[7]Jang, C. S., Ross, J. C., and Cummings, R. M., "Computational Evaluation of an Airfoil with a Gurney Flap," AIAA Paper 92-2708, June 1992.

[8]Janus, M., "Analysis of Industrial Fan Designs with Gurney Flaps," AIAA Paper 2000-0983, Jan. 2000.

[9]Jeffrey, D., Zhang, X., and Hurst, D. W., "Aerodynamics of Gurney Flaps on a Single-Element High-Lift Wing," *Journal of Aircraft*, Vol. 37, No. 2, 2000, pp. 295–301.

[10]Jeffrey, D., "An Investigation into the Aerodynamics of Gurney Flaps," Ph.D. Dissertation, Univ. of Southampton, Southampton, England, U.K., July 1998.

[11]Katz, J., and Largman, R., "Effect of 90 Degree Flap on the Aerodynamics of a Two-Element Airfoil," *Journal Fluids Engineering*, Vol. 111, No. 1, 1989, pp. 93, 94.

[12]Zerihan, J., and Zhang, X., "Aerodynamics of a Single Element Wing in Ground Effect," AIAA Paper 2000-0650, Jan. 2000.

[13]Ranzenbach, R., and Barlow, J. B., "Two-Dimensional Airfoil in Ground Effect, An Experimental and Computational Study," Society of Automotive Engineers, SAE Publ. 942509, 1994.

[14]Ranzenbach, R., and Barlow, J. B., "Cambered Aerofoil in Ground Effect—Wind Tunnel and Road Conditions," AIAA Paper 95-1909, 1995.

[15]Ranzenbach, R., and Barlow, J. B., "Cambered Aerofoil in Ground Effect—An Experimental and Computational Study," Society of Automotive Engineers, SAE Publ. 960909, 1996.

[16]Ranzenbach, R., Barlow, J. B., and Diaz, R. H., "Multi-Element Airfoil in Ground Effect—An Experimental and Computational Study," AIAA Paper 97-2238, 1997.

[17]Burgin, K., Adey, P. C., and Beatham, J. P., "Wind Tunnel Tests on Road Vehicle Models Using a Moving Belt Simulation of Ground Effect," *Journal of Wind Engineering and Industrial Aerodynamics*, Vol. 22, 1986, pp. 227–236.

[18]Moffat, R. J., "Contributions to the Theory of Single-Sample Uncertainty Analysis," *Journal of Fluids Engineering*, Vol. 104, No. 2, 1982, pp. 250–260.

[19]Smith, A. M. O., "High-Lift Aerodynamics," *Journal of Aircraft*, Vol. 12, No. 6, 1975, pp. 501–530.

[20]Bearman, P. W., and Trueman, D.M., "An Investigation of the Flow Around Rectangular Cylinders," *Aeronautical Quarterly*, Vol. 23, Aug. 1972, pp. 229–237.

[21]Gerrard, J. H., "The Mechanisms of the Formation Region of Vortices Behind Bluff Bodies," *Journal of Fluid Mechanics*, Vol. 25, 1966, pp. 401–413.

[22]Bearman, P. W., "On Vortex Street Wakes," *Journal of Fluid Mechanics*, Vol. 28, 1967, pp. 625–641.

A. Plotkin
Associate Editor